

NASA/TM—2004-213057



# Notch Antennas

Richard Q. Lee  
Glenn Research Center, Cleveland, Ohio

---

July 2004

## The NASA STI Program Office . . . in Profile

Since its founding, NASA has been dedicated to the advancement of aeronautics and space science. The NASA Scientific and Technical Information (STI) Program Office plays a key part in helping NASA maintain this important role.

The NASA STI Program Office is operated by Langley Research Center, the Lead Center for NASA's scientific and technical information. The NASA STI Program Office provides access to the NASA STI Database, the largest collection of aeronautical and space science STI in the world. The Program Office is also NASA's institutional mechanism for disseminating the results of its research and development activities. These results are published by NASA in the NASA STI Report Series, which includes the following report types:

- **TECHNICAL PUBLICATION.** Reports of completed research or a major significant phase of research that present the results of NASA programs and include extensive data or theoretical analysis. Includes compilations of significant scientific and technical data and information deemed to be of continuing reference value. NASA's counterpart of peer-reviewed formal professional papers but has less stringent limitations on manuscript length and extent of graphic presentations.
- **TECHNICAL MEMORANDUM.** Scientific and technical findings that are preliminary or of specialized interest, e.g., quick release reports, working papers, and bibliographies that contain minimal annotation. Does not contain extensive analysis.
- **CONTRACTOR REPORT.** Scientific and technical findings by NASA-sponsored contractors and grantees.

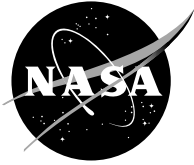
- **CONFERENCE PUBLICATION.** Collected papers from scientific and technical conferences, symposia, seminars, or other meetings sponsored or cosponsored by NASA.
- **SPECIAL PUBLICATION.** Scientific, technical, or historical information from NASA programs, projects, and missions, often concerned with subjects having substantial public interest.
- **TECHNICAL TRANSLATION.** English-language translations of foreign scientific and technical material pertinent to NASA's mission.

Specialized services that complement the STI Program Office's diverse offerings include creating custom thesauri, building customized databases, organizing and publishing research results . . . even providing videos.

For more information about the NASA STI Program Office, see the following:

- Access the NASA STI Program Home Page at <http://www.sti.nasa.gov>
- E-mail your question via the Internet to [help@sti.nasa.gov](mailto:help@sti.nasa.gov)
- Fax your question to the NASA Access Help Desk at 301-621-0134
- Telephone the NASA Access Help Desk at 301-621-0390
- Write to:  
NASA Access Help Desk  
NASA Center for Aerospace Information  
7121 Standard Drive  
Hanover, MD 21076

NASA/TM—2004-213057



# Notch Antennas

Richard Q. Lee  
Glenn Research Center, Cleveland, Ohio

National Aeronautics and  
Space Administration

Glenn Research Center

---

July 2004

Available from

NASA Center for Aerospace Information  
7121 Standard Drive  
Hanover, MD 21076

National Technical Information Service  
5285 Port Royal Road  
Springfield, VA 22100

Available electronically at <http://gltrs.grc.nasa.gov>

# Notch Antennas

Richard Q. Lee  
National Aeronautics and Space Administration  
Glenn Research Center  
Cleveland, Ohio 44135

## Introduction

A notch antenna, also known as tapered slot antenna (TSA), is an end-fire traveling wave antenna. Like microstrip antennas, the TSA features low profile, light weight, easy fabrication by photo-etching, conformal installation and compatibility with microwave integrated circuits (MIC). Performance wise, TSA has demonstrated multi-octave bandwidth, moderate gain (7–10 dB) and symmetric E- and H- plane beam patterns. However, TSA lacks the versatility of microstrip antennas in terms of multifunction operations such as dual-frequency, dual-polarization etc., and loses its planar architecture when used as circularly polarized antennas or in 2-D arrays. The antenna was first proposed by Lewis et al [1] in 1974. Since then, much technological advances have been made in both designs and applications. In designs, various numerical techniques have been developed and applied to aid the design of the TSA antennas [2–4]. Full-wave numerical techniques based on Method of Moments are now commercially available providing the ability to shorten the design cycle as have been demonstrated in a recent CAD benchmark demonstration [5]. In applications, TSAs have been mainly used for spatial-power combining and as focal-plane feed arrays for imaging reflector systems [6–7]. In more recent applications, TSA arrays capable of multi-function operations are emphasized. Examples of these include the dual-band dual-polarized TSA array of nested lattice architecture [8], and multi-frequency full-duplex phased array system with notch elements [9].

This chapter will focus on the most recent advances in TSA and their applications. In order to provide some basic understanding of the design issues, the chapter will begin with some discussions on the design of single tapered slot antennas. Then, TSA arrays and their applications will be highlighted.

## Basic Geometries

A typical TSA consists of a tapered slot section which is produced by the gradual widening of a slot line. The antenna, excited by a slotline feed, is fabricated on a metallization layer with or without a supporting dielectric substrate. The tapered slot section which constitutes the radiating region can take on any of three geometric profiles: (1) nonlinear taper (Vivaldi, tangential or parabolic), (2) linear taper (LTSA), and (3) constant width (CWSA) [10]. The majority of previous studies have been focused on TSA with linear and exponential profiles. Prasad and Mahapatra [11] first introduced the linearly tapered slot antenna (LTSA) in 1979. Their antenna of about one free space wavelength long was etched on a 25-mil alumina substrate. In the same year, Gibson [12] reported a TSA with exponentially tapered profile, also known as “Vivaldi” antenna, which demonstrated a bandwidth of 8–40 GHz. The schematics of the LTSA and the Vivaldi antennas are shown in fig. 1. In later years, most of the subsequent developments of TSA arrays are derived mainly from these two antenna types.

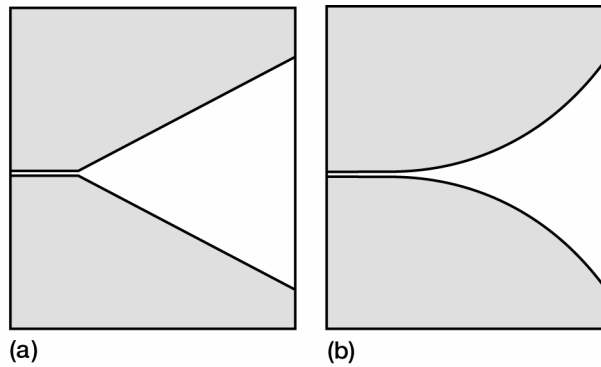


Figure 1.—Schematics of antennas. (a) LTSA. (b) Vivaldi.

In order to facilitate integration of antenna and devices at sub-millimeter wave frequencies, a new variant of the TSA, generally known as V-antennas, was introduced in 1979 for coupling radiation into diode mixers [13]. Years later, other applications of V-antennas were demonstrated at microwave frequencies [14–15]. These antennas with finite width ground planes can enhance the antenna performance by suppressing the surface waves. Another advantage of the V-antennas is its compatibility with uniplanar feed structures which allow to excite the antenna with either a microstrip line or a waveguide [14]. The schematics of a V-LTSA and a V-Vivaldi excited by a coplanar stripline are shown in fig. 2.

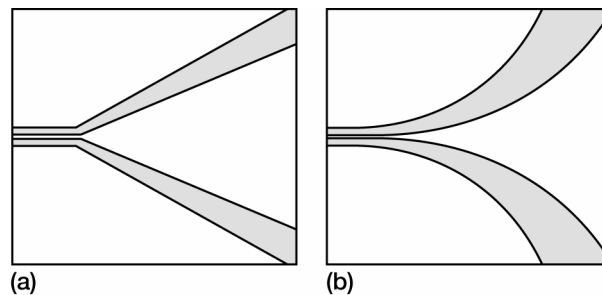


Figure 2.—Schematics of V-antennas. (a) V-LTSA. (b) V-Vivaldi.

Another variant of the conventional TSA is the antipodal tapered slot antenna. In practice, the conventional planar TSA is fed by a balanced slotline. One serious drawback of the conventional TSA is in the fabrication and impedance matching of the slotline. Slotline fabricated on a low dielectric constant substrate has relatively high impedance which makes matching to a microstrip feed very difficult. The antipodal TSA is designed to overcome this impedance matching difficulty; however, it has exhibited very poor cross-polarization characteristics. The antenna is formed by gradually flaring the strip conductors of the balanced microstrip on opposite sides of the dielectric substrate with respect to the antenna axis, thus allowing the antenna to be directly fed by a microstrip feed [16]. To circumvent the high cross-polarization problem, a balanced antipodal Vivaldi consisting of three metallization layers was introduced. This new antenna, shown in fig. 3, has demonstrated  $-15$  dB lower cross-polarization across a 18:1 band as compared to the conventional Vivaldi antenna [17].

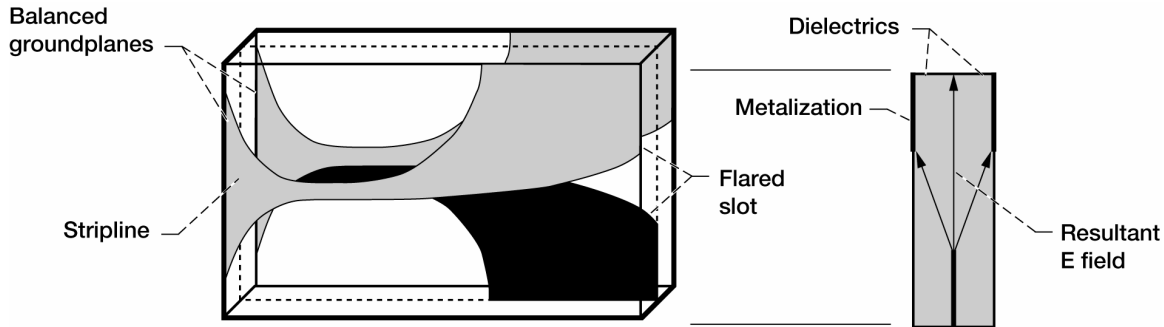


Figure 3.—Balanced antipodal Vivaldi antenna. From ref. 17 with permission from IEEE.

## TSA Design

For years, the design of TSA has been primarily based on empirical approach, which as an initial step, could start with the following simple guidelines:

The aperture width of slot:  $W \geq \lambda_0$

$$1.05 \leq c/v \leq 1.2$$

The effective thickness:  $t_{eff} \leq .03 \leq \lambda_0$

The taper angle,  $2\alpha$ , is typically 5 to 12°

The length of the TSA,  $L$ , is typically 2 to 12  $\lambda_0$

where  $c$  is the velocity of light,  $v$  is the velocity of the field along the slot, and  $\lambda_0$  is the free-space wavelength. With the availability of electromagnetic simulators, engineers can now check the accuracy of their designs before carrying out the actual fabrication and characterization. In general, the design of TSA involves two major tasks: (1) the design of a broadband transition and feed structure with very wide frequency range and low return loss, and (2) determining the dimensions and shape of the antenna in accordance with the required beamwidth, side lobe, and back lobe etc. over the operating frequency range. The geometric parameters such as length, width, dielectric thickness, ground-plane size, and taper-profile which have direct impact on the impedance, directivity, bandwidth, and radiation pattern of the antenna will be discussed in the sections below.

## Feeding Methods

Almost always planar tapered slot antennas such as LTSA and Vivaldi are excited by a slotline; thus, feeding a TSA requires building a transition between the slotline and other transmission media. In the case of microstrip or coaxial lines, the transition is a balun. In general, the transition should have small parasitic inductance and capacitance for wide bandwidth, and hence, electromagnetic coupling is preferred over wire bonding or solder connection. In the following, we will consider three basic feed structures: (1) coplanar waveguide (CPW), (2) microstrip line, and (3) coaxial lines.

*Coplanar Waveguide-Feed:* CPW possesses many useful design characteristics such as low radiation loss, less dispersion and uniplanar configuration. In [10], we have presented several feeding techniques where the transmission media are CPW which excite the TSA via electromagnetic coupling. Figure 4(a) shows a strip-to-slot coupled LTSA excited by a conductor-backed finite ground-plane CPW feed. This antenna has demonstrated a VSWR of 2:1 over nearly 3:1 bandwidth as indicated by the measured return loss shown in fig. 4(b).

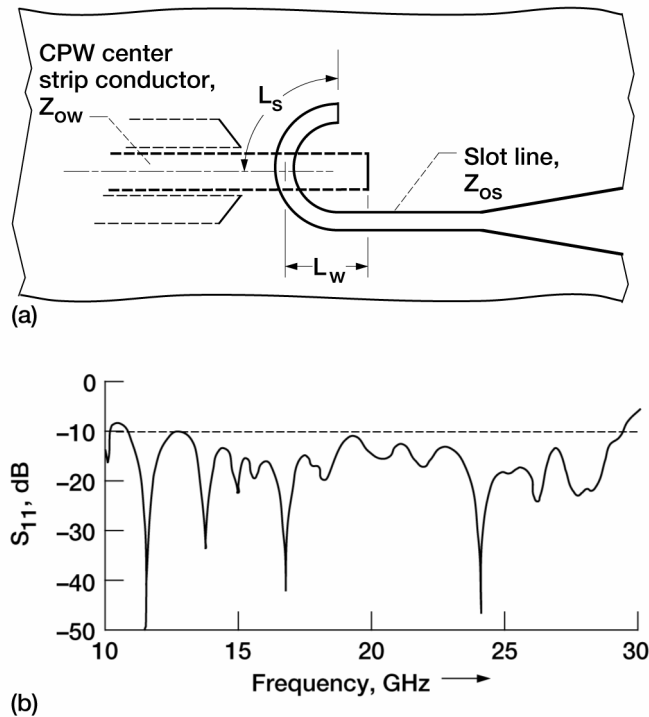


Figure 4.—Strip-to-slot coupled LTSA. (a) CPW strip-to-slot transition. (b) Measured return loss.

The TSA can also be excited by direct slot-to-slot feeding where the CPW and the antenna are on the same side of the substrate. In order to excite the odd mode where the electric fields in both slots of the CPW have the same amplitude but opposite direction, a bondwire is usually placed across the slots to keep the two ground planes at equal potential. The CPW feed enables direct integration of active solid state devices with the antenna. Figure 5 shows a LTSA integrated with a FET amplifier which demonstrated a gain of more than 14 dB over a bandwidth of 1.75 GHz [18].



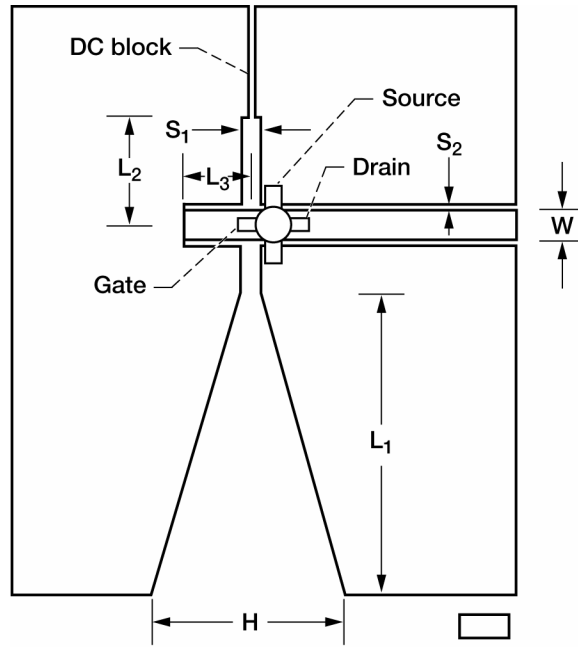


Figure 5.—Circuit configuration of CPW cross-feed LTSA amplifier. From ref. 18 with permission from IEEE.

CPW can be designed as a tapered CPW with constant characteristic impedance, but with different ratio of slot to center strip widths [19]. This unique feature is useful for exciting twin tapered slot antennas of large separations.

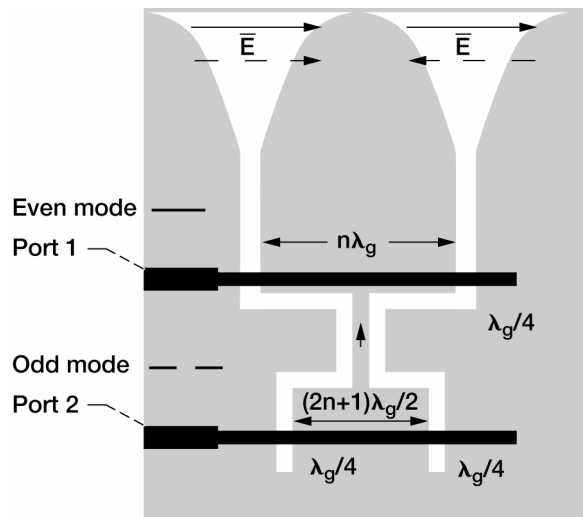


Figure 6.—Twin LTSAs fed with tapered CPW transitions.

Figure 6 shows the application of tapered CPW transitions to twin Vivaldi antennas to achieve pattern diversity for transponders and monopulse systems through even and odd mode excitations [20]. With this approach, exciting the even mode produces a maximum radiation, while exciting the odd mode produces a minimum radiation in the boreside direction.

**Microstrip Line Feed:** Microstrip line is in widespread use in power combining circuit. Since microstrip line is an unbalanced line and slotline is a balanced line, feeding a TSA with a microstrip line requires a balanced-to-unbalanced transition (balun) to avoid compromising the broadband antenna performance. The most common microstrip/slot transition, the Marchand balun [21], has demonstrated a VSWR of 2:1 over an octave bandwidth with an integrated wideband V–Vivaldi antenna [22]. The transition and the corresponding transmission line model are shown in fig. 7. The balun consists of four quarter-wave sections with the end open-circuited section extended past the center of the slotline by about one quarter of a guided wavelength. Further broadening of the bandwidth can be achieved when the microstrip is terminated by a radial stub and the slot line is terminated by an elliptical shaped cavity [10].

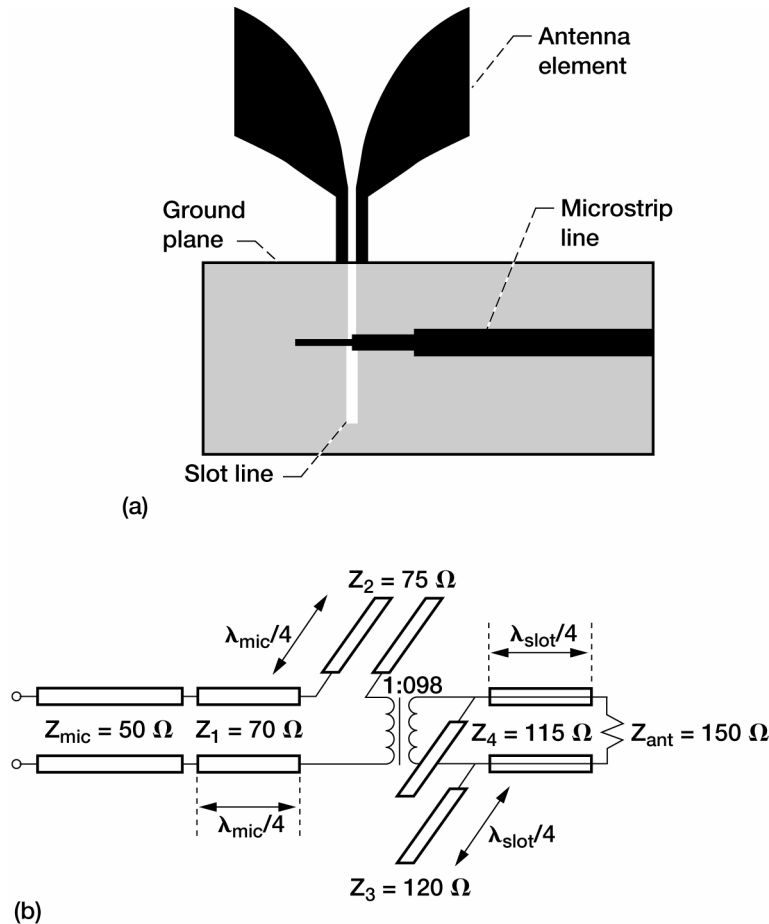


Figure 7.—Schematic of Marchand balun. (a) With interface to antenna element. (b) Transmission line model. From ref. 22 with permission from IEEE.

The double-Y balun is another microstrip-to-slotline transition which has no inherent bandwidth limitation other than parasitic inductances and capacitances. As indicated in fig. 8, the double-Y balun is based on the 6-port double-Y junction which consists 3 balanced and 3 unbalanced lines placed alternately around the center of the structure. For the balun to provide perfect transmission between an opposite balanced and unbalanced ports, opposite pairs of lines should have reflection coefficients with opposite phases; thus requiring one pair of lines to be short circuit while the other open circuit. TSA with double-Y balun feed structure has achieved an impedance bandwidth of more than 2:1 [23].

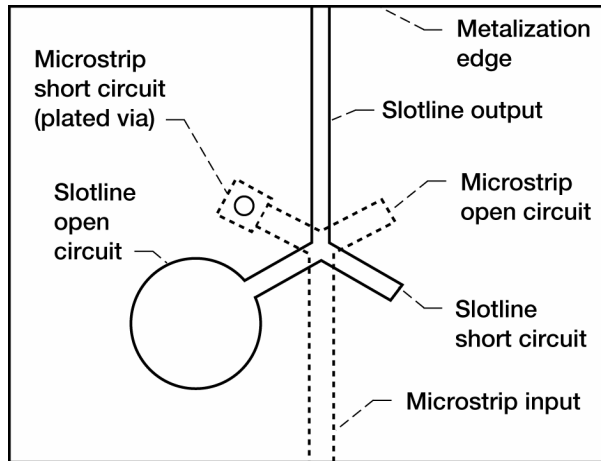


Figure 8.—Double-Y microstrip-to-slotline transition.

The balun requirement often complicates the feed design and limits the antenna bandwidth if it is not designed properly. The V- and antipodal tapered slot antennas offer a way to circumvent this problem since they are not directly fed by a slotline. Figure 9 shows a V-LTSA with a uniplanar microstrip-to-coplanar stripline feed [24]. In the feed network, a microstrip line of characteristic impedance of  $50\ \Omega$  and width  $W_1$  is coupled to two orthogonal microstrip lines of characteristic impedance of  $70\ \Omega$  and width  $W_2$  through a quarter-wave impedance transformer of width  $W_1$ . The mean path length of the folded loop “a through b” is equal to half a guide wavelength  $\lambda_g$  of the  $70\ \Omega$  microstrip line at the design frequency. However, for wideband operation, the mean path length needs to be increased to  $0.638\ \lambda_g$  to compensate for the right-angle bend parasitic elements. This design ensures that the signal phase from points “a” to “b” are 180 degree out of phase; thus the coupled microstrip lines are excited in the odd mode with the electric field predominantly across the gap  $S_2$ . The dimension of  $S_2$  is chosen such that the characteristic impedance of the coupled microstrip line is  $50\ \Omega$ . The measured return loss of the V-LTSA is better than 10dB over the frequency range of 5 to 15 GHz.

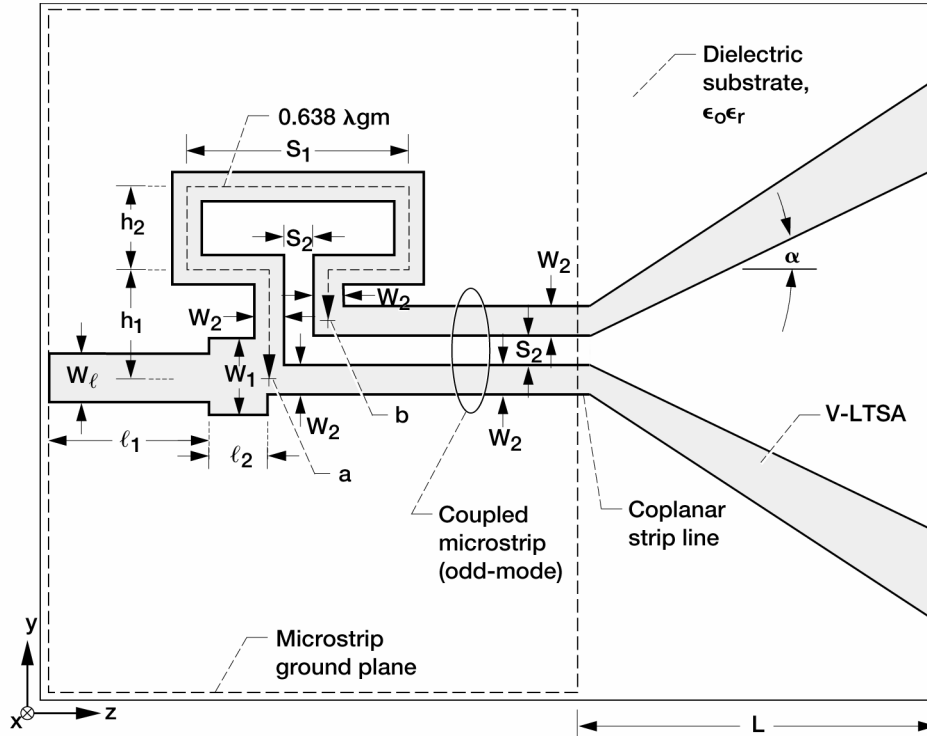


Figure 9.—V-LTSA with a uniplanar microstrip line-to-coplanar stripline feed,  $\alpha = 12.5^\circ$  and  $L = 2$  in.

Figure 10 shows an antipodal LTSA with a microstrip-to-balanced microstrip feed. The balanced microstrip is formed with the ground plane tapered to a width equal the strip width  $W_1$  and the radius  $R_2$  of the arc is arbitrarily chosen to provide a smooth taper transition for matching the characteristic impedance of the conventional microstrip to the balanced microstrip.

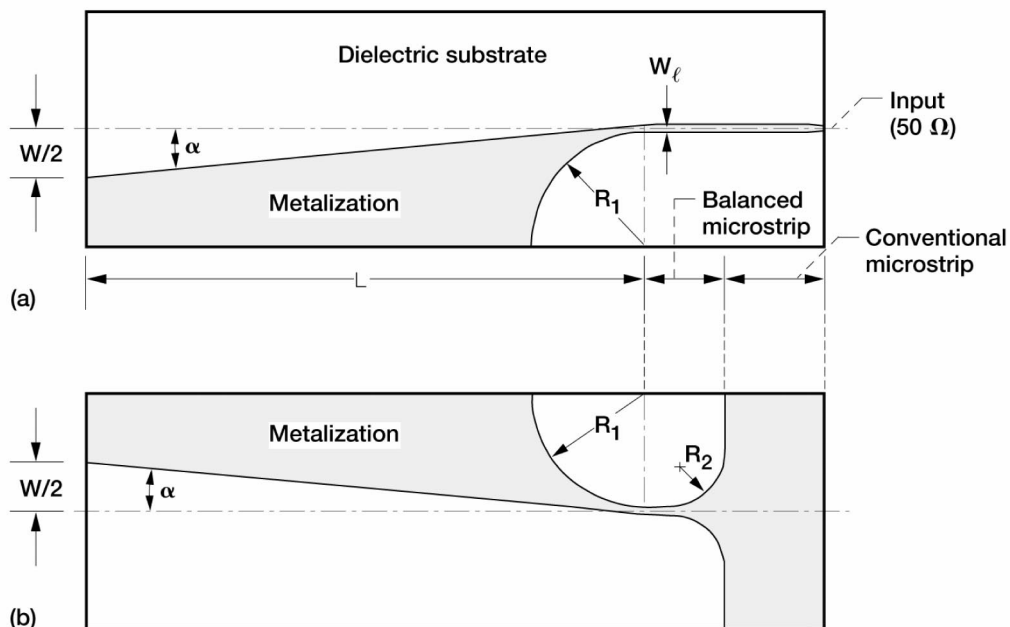


Figure 10.—Antipodal LTSA and feed network. (a) Top metalization. (b) Bottom metalization.

The electric field lines at different cross section along the feed and the antenna are illustrated in fig. 11. The electric field lines which are spread out in the conventional microstrip structure concentrate between the metal strip of the balanced microstrip, and finally rotate while traveling along the LTSA. The field rotation inadvertently introduces higher cross-polarizations in these types of antennas. The antipodal LTSA has demonstrated over 4:1 (8–32 GHz) bandwidth for 2:1 VSWR at the design frequency of 18 GHz [25].

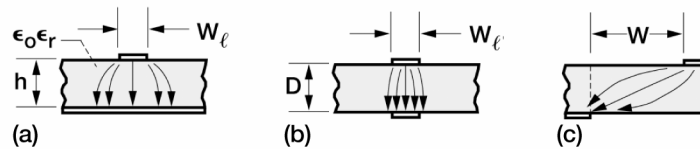


Figure 11.—Electric field distribution at cross sections.  
 (a) Conventional microstrip. (b) Balanced microstrip.  
 (c) Antenna radiating edge.

**Coaxial feed:** Coaxial line is useful as a feed structure because of its compatibility with the slotline, coplanar microstrip, or balanced microstrip to form wideband transitions; thus, it can be used to excite all three variants of TSA described above. The disadvantage is that it is not planar and has high losses at high frequencies. Further, coaxial line is an unbalanced feed line. All of the currents flow inside the line, i.e. the inner conductor and the inside of the shield. Feeding a balanced antenna with unbalanced coaxial feed may cause currents to flow on the outside of the shield, which could result in significant power loss and serious distortion in radiation pattern. Since the magnitude of the current on the outside shield is a function of the impedance to ground of the conductor, one common approach to cutoff the flow of current is with an open circuit which is created by placing a “skirt” one quarter of a wavelength long around the outside shield and shorted to the shield at one quarter of a wavelength away from the load.

The most direct way of exciting a TSA with a coaxial feed is to extend its center conductor over the slotline section of the TSA and anchor the coaxial feed with solder connection to the ground plane. Recently, an improved balun design which has direct application to V-antennas has been proposed [26]. The balun impedance is tapered by cutting open the outer wall of the coax so that the reflections at the input are minimized. The length of the balun is determined by the lowest operating frequency and the maximum reflection coefficient which occurs in the passband. Figure 12 shows the cross-section of the tapered coaxial line balun and its integration with a V-Vivaldi antenna.

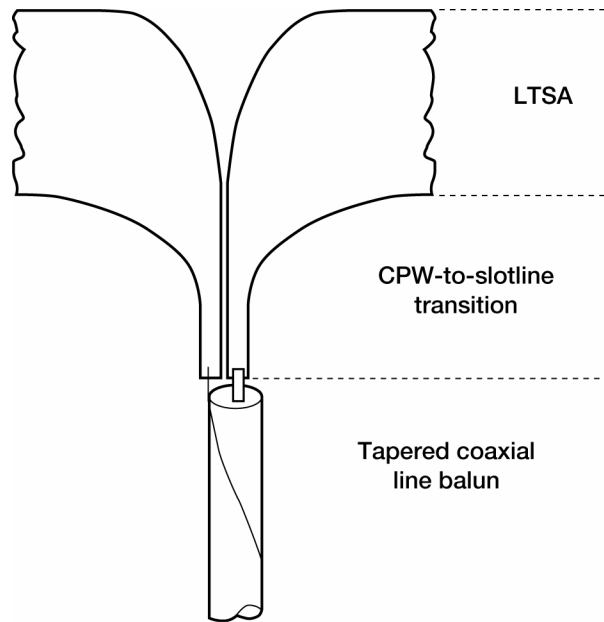


Figure 12.—Coaxially-fed TSA with tapered coaxial line balun. From ref. 26 with permission from IEEE.

## Radiation Characteristics

A good understanding of the effects of the design parameters (length, width, dielectric thickness, ground-plane size and taper profile etc.) on antenna characteristics would facilitate the task of antenna design. TSA is known to have good performance over a wide bandwidth. In practice, the operating bandwidth is often limited by the slotline-to-feedline transition and by the finite width of the antenna. To achieve wideband operation requires the TSA to operate in a traveling-wave mode with perfect impedance match at both the feed transition and the slot termination. In this section, some important characteristics of TSA, which are based on experimental data as well as from previous publications, will be presented.

*Effect of length, width and taper profiles:* Tapered slot antennas radiate in the endfire direction with fairly symmetric radiation patterns, but have high cross-polarization levels in the diagonal plane. The lowest cross-polarization level in the diagonal plane is about 10 to 15 dB higher than that of the principal planes which are typically better than  $-15$  dB. In general, the cross-polarization characteristics of planar TSA are superior to those corresponding to their antipodal counterparts.

Being a traveling wave antenna, the phase velocity and guide wavelength,  $\lambda_g$ , varies with any change in the geometrical and material parameters of the antenna, which in turn impacts the radiation characteristics of the antenna. The gain of a TSA increases with the length,  $L$ , of the antenna typically from a few dB to over 10 dB as  $L$  increases from  $2-5\lambda_g$  [10]. Maximum measured gain of 16–17 dB with radiation efficiency of 80 percent has been reported for long TSA with  $L$  greater than  $6\lambda_0$  [27]. Similarly, the beamwidths, being inversely proportional to gain, decrease rapidly as the length is increased; however, the H-plane beamwidth varies more slowly in comparison to the E-Plane beamwidth particularly for  $L$  less than  $5\lambda_g$ .

The taper profile has been found to have strong effects on both the beamwidth and sidelobe level of the antenna. In general, the beamwidths are narrower for the CWSA, followed by the LTSA, and then Vivaldi for antennas with the same length, same aperture size, and on the same substrate. Similarly, the sidelobes are highest for the CWSA, followed by the LTSA, and the Vivaldi.

As a traveling wave antenna, the H-plane beamwidth follows  $1/\sqrt{L}$  dependence, while the E-plane beamwidth depends more on the aperture width or tapered angle [28]. Varying the tapered angle will change the phase velocity and hence  $\lambda_g$ , which will in turn change the E-plane beamwidth. Thus, constant beamwidth in both E- and H-plane can be achieved with proper choices of  $L$  and tapered angles. Gibson obtained approximately constant beamwidth in both E- and H-plane for a Vivaldi antenna fabricated on alumina substrate with tapered profile defined by [12].

$$y = \pm 0.125\exp(0.052x)$$

Recently, approximately constant E- and H-plane beamwidths over a 6 to 18 GHz bandwidth was demonstrated for a balanced antipodal antenna with elliptical radiating taper [17], and nearly identical E- and H-plane 3-dB beamwidth was observed for a LTSA with tapered angles in the range of 15 to 20 degrees [29].

*Effect of dielectric:* The performance of a TSA is sensitive to the thickness and dielectric constant of the dielectric substrate. The presence of a dielectric substrate has the primary effect of narrowing the main beam of the antenna. The effects of dielectric substrates on the E- and H-plane beamwidths of a Vivaldi antenna on polyethylene have been investigated at 18.5 GHz [30]. By varying substrate thickness from 10 to 15 and 27 mils, the H-plane beamwidths become narrower, while the E-plane beamwidths remain essentially constant, indicating that the dielectric has a strong effect on the H-fields. Increasing the dielectric thickness generally results in increased gain, but with higher sidelobes. For good performance, a TSA should have an effective substrate thickness in the range of  $0.0025\lambda_0 \leq t_{eff} \leq 0.028\lambda_0$  where  $t_{eff} = t(\sqrt{\epsilon_r} - 1)$  is the effective thickness of the substrate. For substrate thickness above the upper bound of  $0.028\lambda_0$ , unwanted substrate modes develop which degrade the antenna performance resulting in low efficiency and narrow bandwidth, particularly for dielectrics with high dielectric constants. Further, for millimeter-wave operations, the upper bound on the effective thickness constrains to using mechanically fragile substrates with thickness of only a few hundreds of microns. To overcome these problems, it has been proposed to fabricate notch antennas either on thick perforated substrates with an array of regularly and closely placed holes [31] or on photonic bandgap dielectrics as shown in fig. 13 [32]. The former approach reduces the effective substrate thickness, while the latter approach suppresses the excitation of the surface modes.

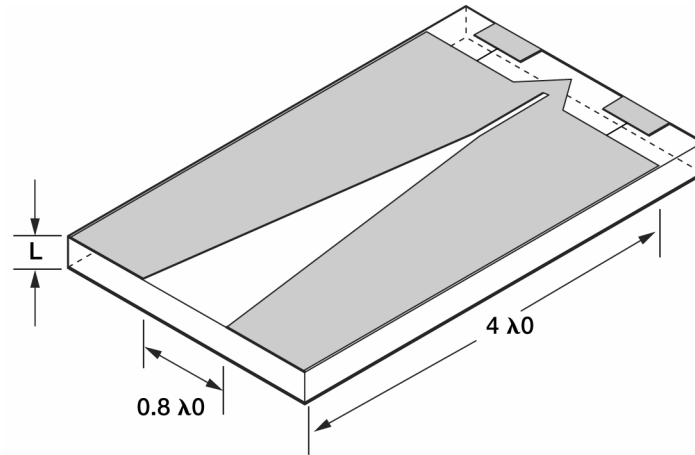


Figure 13.—Micromachined tapered slot antenna. From ref. 32 with permission from IEEE.

*Ground Plane Effect:* Placing a ground plane immediately below the TSA will cause the main beam to steer away from the endfire direction by about  $50^\circ$  in the H-plane [10]. The amount of scan will be reduced as the distance between the ground plane and the antenna increases, and becomes negligible when the distance of separation is sufficiently large. For the E-plane patterns, no significant change was observed except that the TSA had to be tilted in the elevation to receive full power. Figure 14 shows measured H-plane patterns for a LTSA over a ground plane with a foam spacer in between.

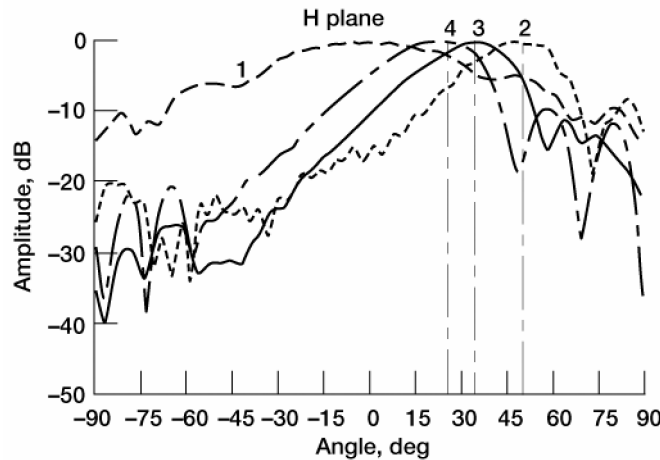


Figure 14.—H-plane patterns at 11 GHz for a LTSA with a foam spacer. (1) With no ground plane. (2) With a ground plane and no spacer. (3) With a ground plane and a 0.3175-cm foam spacer. (4) With a ground plane and a 0.635-cm foam spacer.



## Impedance Characteristics

**Input impedance:** The impedance characteristic of TSA is important for designing match transitions; yet very little information is available from previous publications. Based on conformal mapping method for a fin antenna without a dielectric, Yngvesson et al. reported that the impedance of a LTSA with thin dielectric is essentially constant at frequencies from 4 to 12.4 GHz and is close to  $80 \Omega$  [33]. In a recent study, the input impedance of LTSA was measured using a microwave wafer probe and a set of on wafer Thru-Reflect-Line (TRL) slotline standards [34]. The LTSA was excited through a short length of a slotline by a ground-signal microwave probe (Picoprobe, Inc.). In the measurement, the reflection coefficient of the LTSA is de-embedded from the measured reflection coefficient at the input terminal of the slotline using the NIST de-embedded software [35]. Figure 15 shows the real and imaginary parts of the input impedance,  $Z_{in}$ , versus frequency for a LTSA with  $\alpha = 5^\circ$  and  $L = 2.54\text{cm}$ .

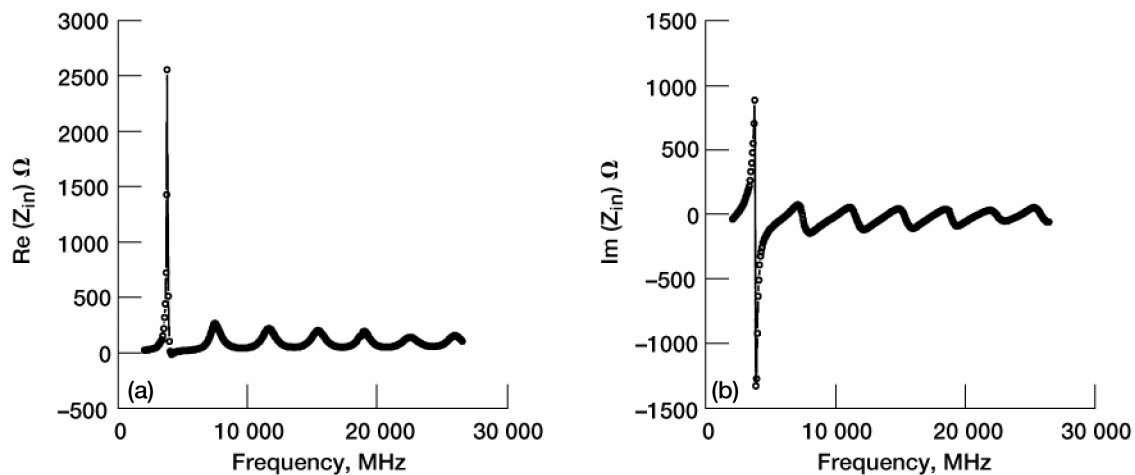


Figure 15.—Real and imaginary parts of the input impedance,  $\alpha = 5^\circ$  and  $L = 2.54 \text{ cm}$ . (a) Real. (b) Imaginary.

The impedance plot exhibits a series of resonance over the frequency band from 2 to 26.5 GHz. These resonances are caused by imperfect impedance match transitions at the feed end and the termination end of the LTSA. The first resonance mode at frequencies below 4 GHz has very large input impedance, typically over  $1000 \Omega$ , which could be caused by large electric fields associated with a very small  $W/\lambda_0$ . For frequencies above 4 GHz, the impedances are bounded between  $145 \Omega$  and  $40 \Omega$  with a mean value of about  $92 \Omega$ . Similar results were also obtained for LTSA of different lengths and tapered angles [10].

**Impedance matching:** Impedance matching of TSA has commonly been performed at the feed end of the antenna. Recently, an approach illustrated in fig. 16 for impedance matching at the termination end of the antenna has been proposed [36].

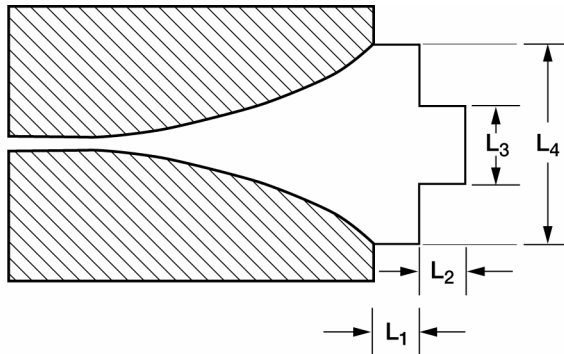


Figure 16.—Vivaldi antenna with a dielectric impedance matching transformer.  $L_1 = 4$  mm,  $L_2 = 4$  mm,  $L_3 = 5$  mm, and  $L_4 = 10$  mm.

The new approach uses a two-step dielectric transformer to match the antenna to free space. The de-embedded real and imaginary parts of the input impedance with and without the dielectric transformer are shown in fig. 17.

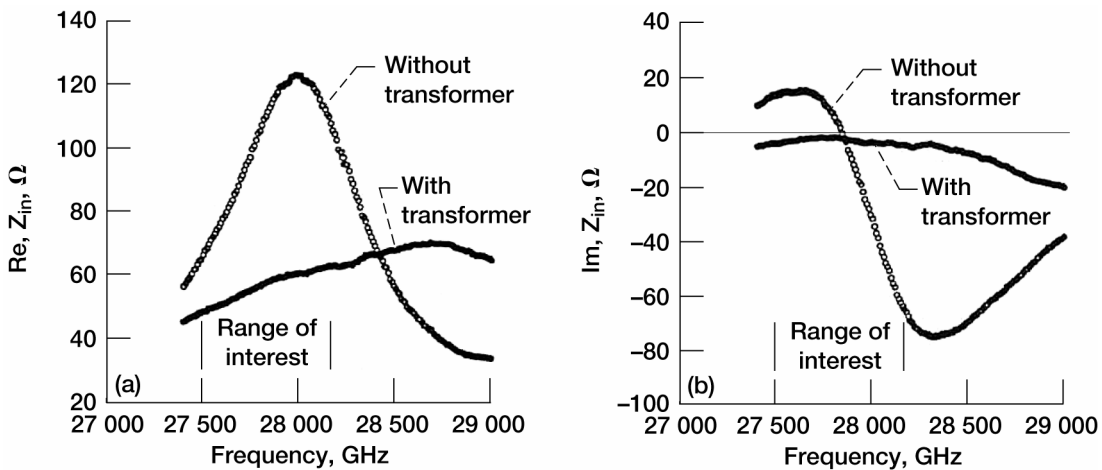


Figure 17.—Real and imaginary parts of the input impedance. (a) Real. (b) Imaginary.

*Mutual impedance:* Mutual coupling can produce profound impacts on the performance of an antenna array causing impedance mismatch and scanning blindness particularly for antennas on thick dielectric substrates. In general, mutual coupling can occur between two TSAs arranged either in coplanar or stacked configurations. Recently, the mutual coupling between two LTSAs in close proximity and excited by two calibrated ground-signal microwave probes was obtained from an S-parameter measurement of  $|S_{21}|$  [37]. Figure 18 shows the measured mutual coupling between two LTSAs in coplanar and stacked arrangement as a function of separations. Results indicate that the mutual coupling decreases with the distance of separation.

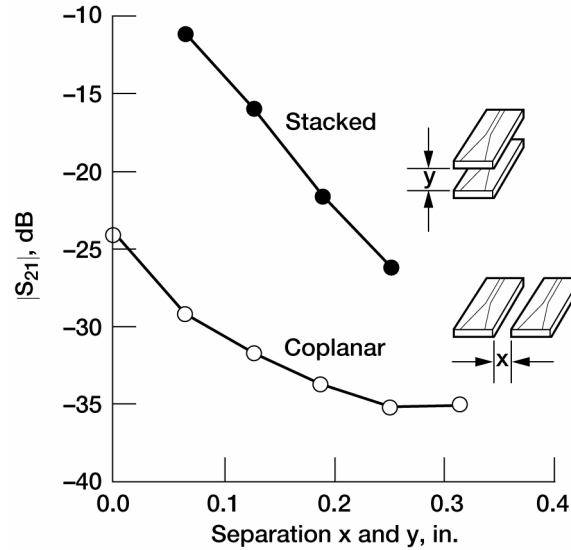


Figure 18.—Measured mutual coupling between two LTSAs in coplanar and stacked arrangements as a function of separation.

The coupling coefficients as a function of frequencies were also measured first with the LTSAs fabricated on a continuous substrate and then repeated after a narrow slot was cut in the dielectric. In the latter case, coupling between antennas were confined to space waves only. Results indicate stronger mutual coupling for the TSAs on continuous substrate as a result of additional coupling through the supporting dielectric; however, both cases display decreasing  $|S_{21}|$  with frequencies [10]. This is due to the fact that at higher frequencies the separation is electrically larger and separations between antennas are greater with respect to wavelengths.

## TSA Array and Applications

Over the years, many different applications of TSA arrays have been reported in the literature. TSA arrays have been successfully applied as focal plane feed arrays for a multi-beam imaging reflector system. For the same beamwidth, a TSA array occupies about 1/4 of the area of a feed array with waveguide elements; thus, imaging system with TSA focal plane array can be designed to yield high angular resolution [27].

TSA arrays have also been advantageously used for spatial power combining to achieve power amplification and harmonic generation. Recently, a 120-watt, X-band spatially combined solid-state amplifier has been demonstrated [6]. The spatial combiner consists of six identical “trays” with each containing four input/output broadband TSA integrated with four MMIC amplifiers via a slot-to-microstrip transition. Space power combining can be applied to large antenna aperture such as space-fed lens arrays. The concept of space power amplification has been demonstrated experimentally with a three-element LTSA array module. Figure 19 shows a photo of the array module and the measured H-plane pattern.

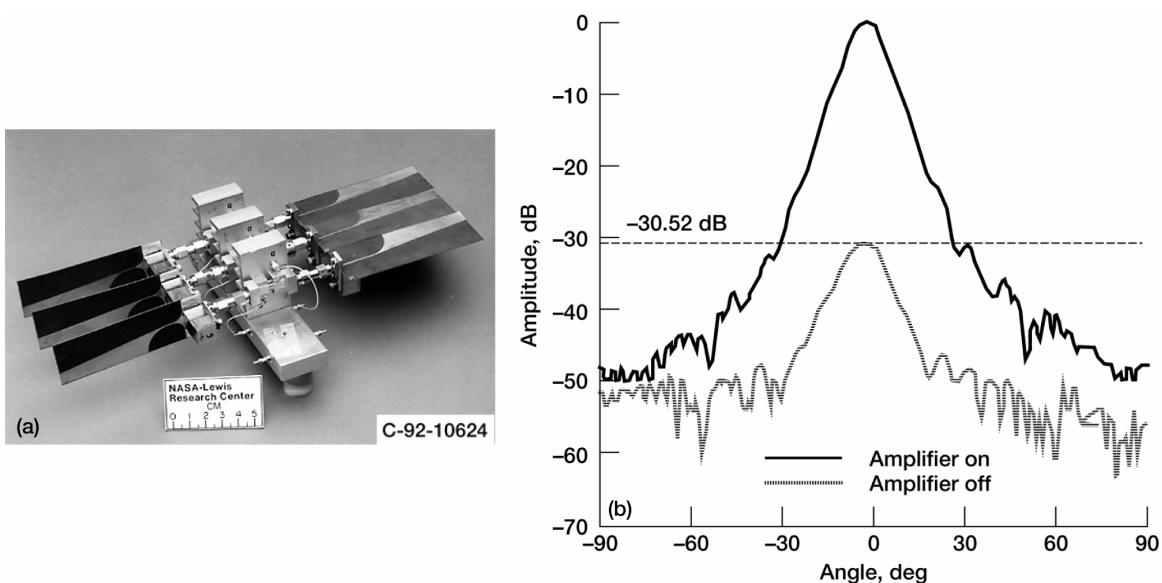


Figure 19.—Experimental three-element LTSA MMIC array module for space power amplification. (a) Photo of module. (b) Measured H-plane pattern.

In this approach, an array of active antenna modules, constructed from non-planar TSA's and monolithic microwave integrated circuit (MMIC) multistage GaAs power amplifiers, receives the signal at lower power and after amplification re-radiates the signal into free space. Polarization diversity is employed to permit accurate measurement of the amplified signal radiated from the transmitting array. With the amplifiers turned on, the three-element active array module produced a gain of 30 dB at 20 GHz [38]. Replacing the MMIC multistage power amplifier with a broadband, GaAs MMIC distributed amplifier, frequency multiplication and space power combining was demonstrated with the same active LTSA array module which receives signal at 9.3 GHz, and after amplification, radiates the second harmonic signal into free space. Results indicated a fundamental-to-second-harmonic conversion efficiency of 8.1 percent [39]. For experimental details and measured results, the reader is referred to reference [10].

With the rapid development of the wireless industry in recent years, a K-band circular LTSA array, shown in fig. 20, has been proposed for mobile communications [40]. The 16-element array is fed by a 1:16 microstrip line power splitter composed of T-junctions and right-angle bends. The output

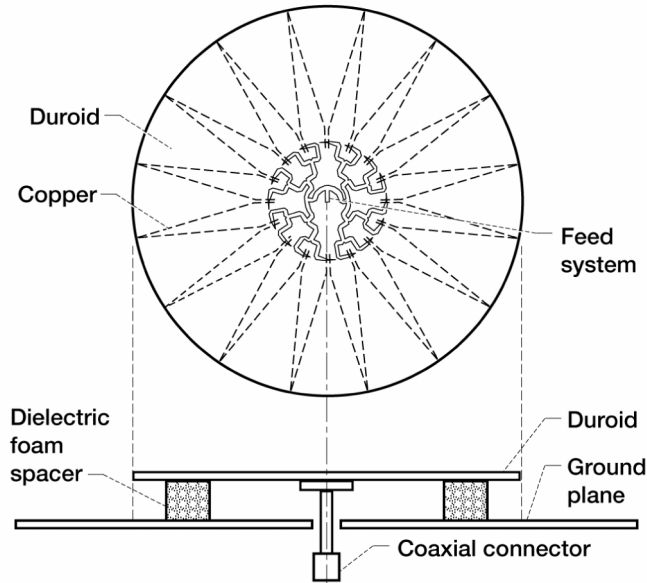


Figure 20.—16-element circular LTSA array.

ports of the splitter are electromagnetically coupled to the slotline of the LTSA through a microstrip-to-slotline transition with the slotline and microstrip line characteristic impedances chosen to be  $120 \Omega$  and  $100 \Omega$  respectively. The array was placed over a reflecting ground plane to displace the beam above the horizon, and foam spacers of different thickness are used to control the amount of scan. Figure 21 shows the measured E- and H-plane patterns for  $0.286\lambda_0$  separation. As shown, the circular LTSA array produces an omnidirectional pattern in the azimuthal plane and a beam displacement of about  $28^\circ$  in the elevation plane.

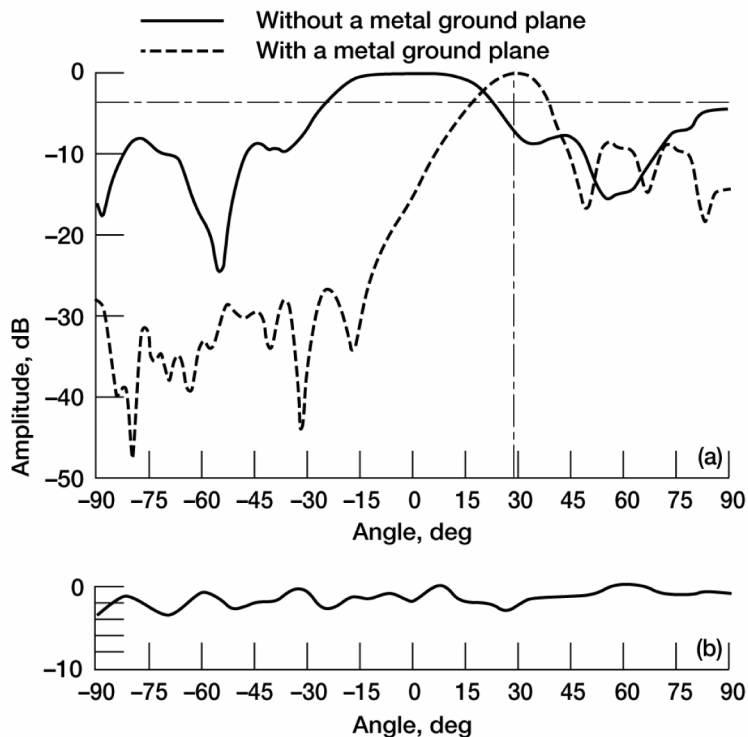


Figure 21.—Measured patterns at 19 GHz. (a) H-plane. (b) E-plane.

Using a similar approach, an omni-directional quasi-optical circular array of 12 Vivaldi-coupled oscillator elements has been designed for LMDS (Local Multipoint Distribution Services) applications [41]. The array, which is powered from a single direct-current power supply, has demonstrated an 87 percent power combining efficiency, and 144 mW radiated power at 28 GHz.

TSA array has found applications in intelligent transportation systems. A wide-scan spherical-lens antenna at millimeter-wave frequency (77 GHz) was recently introduced for automobile radars [42]. The multibeam antenna system is composed of planar TSA which are positioned around a homogeneous spherical Teflon lens. Beam scanning is achieved by switching between elements. Figure 22 shows a 33-beam spherical Teflon lens system which has demonstrated an angular resolution of  $5.5^\circ$  and  $-3.5$  dB crossover of adjacent beams.

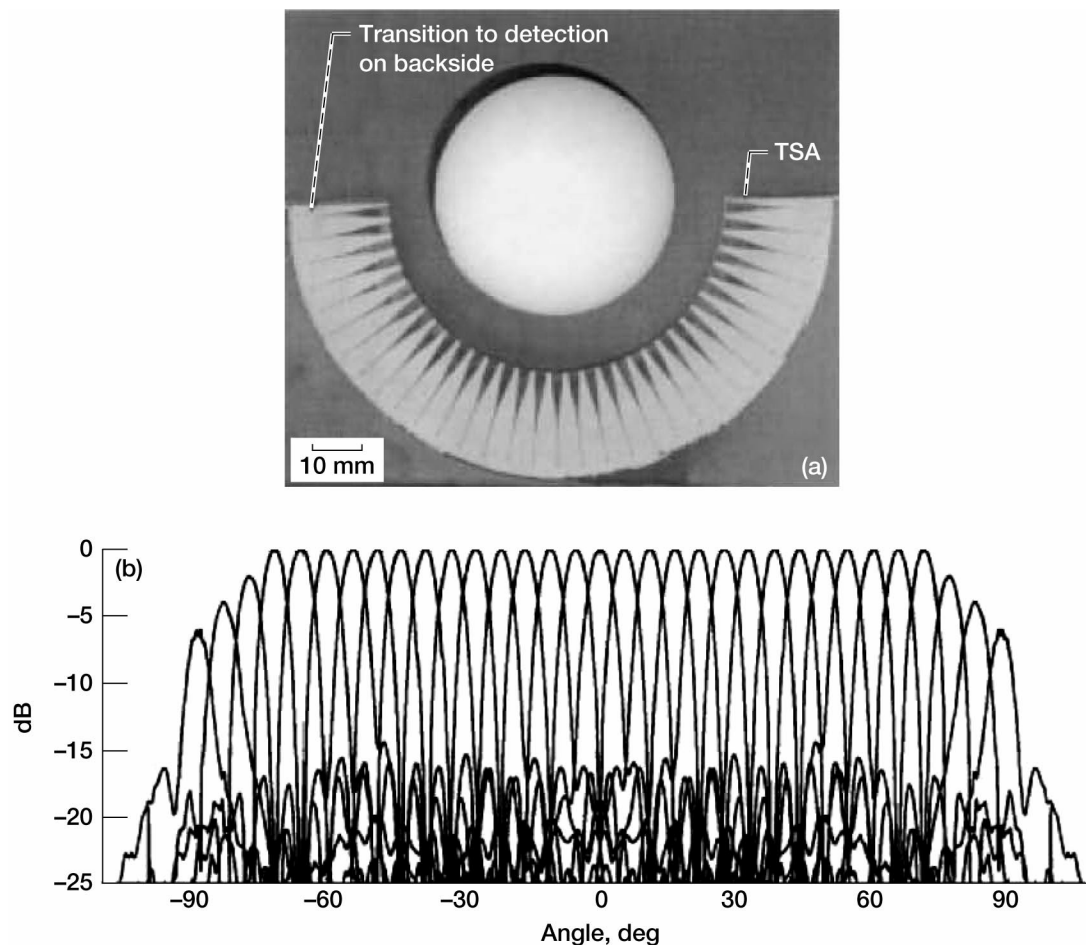


Figure 22.—33-beam array with spherical Teflon lens. (a) Photo of array. (b) Measured E-plane pattern. From ref. 42 with permission from IEEE.

In shared aperture technology development where the functionality of several antennas are combined into one aperture using wideband multiple beam technology, dual-polarized tapered slot antennas with “double Y” microstrip-to-slotline transition have been used to achieve wideband operations [43]. To realize horizontal and vertical linear polarization, two TSA elements of like polarization are first combined into a two-element subarray. Then, two such subarrays are joined at  $90^\circ$  through a mechanical slot cut in the top of one subarray and the bottom of the other subarray

to form a quad-element subarray module. Figure 23 shows an 8×8 array composed of quad-element subarray modules as building blocks. To obtain right- and left-hand circular polarization, the horizontal and vertical polarizations are combined with a 90° phase-offset in a quadrature hybrid circuit.

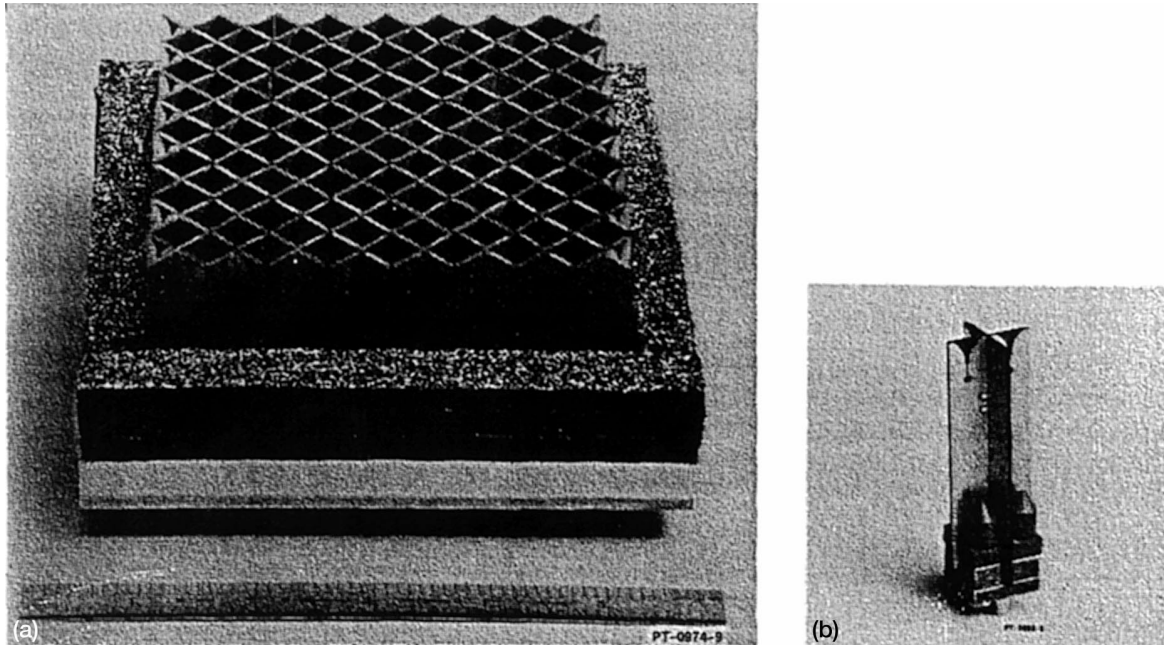


Figure 23.—Photographs of dual-polarized TSA array. (a) 8×8 array. (b) Orthogonal subarray element pair.

Combining the functionality of several antennas into one shared aperture presents many technical challenges. Recently, a dual-band dual-polarized nested antipodal Vivaldi array has been developed for a new radio-telescope, the Square Kilometer Array (SKA) [8]. In order to meet the 5:1 bandwidth (0.8 to 4.0 GHz) requirement, the array consists of a lower-band and an upper-band subarray with each made up of different-size antipodal Vivaldi quad-elements having overlapping bandwidths. The array of nested lattice architecture has multilevel ground planes which allow height-adjustment to achieve optimization of the array performance. A sketch of a 20-element dual-band dual-polarized multilevel nested antipodal Vivaldi array is shown in fig. 24.

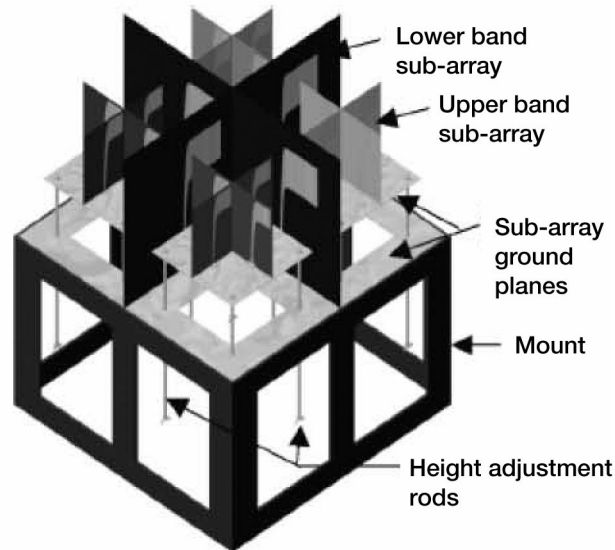


Figure 24.—Sketch of a 20-element dual-band dual-polarized multilevel antipodal Vivaldi array. From ref. 8 with permission from IEEE.

In a recent development of a low-cost, multi-frequency and full-duplex phased array transceiver that transmits at 10 or 19 GHz and receives at 12 or 21 GHz, Vivaldi antennas were used to achieve wide-band performance. In addition, the system, as illustrated in fig. 25, features a low-loss and low-cost multi-line phase shifter controlled by dual piezoelectric transducers (PET) and four-channel microstrip multiplexers [9]. The array system has demonstrated scan angles of about 40° at 10 to 21 GHz using the PET phase controls. The use of PET greatly simplifies the integration and high insertion loss problems generally associated with solid-state type phased shifters used in conventional phased arrays.

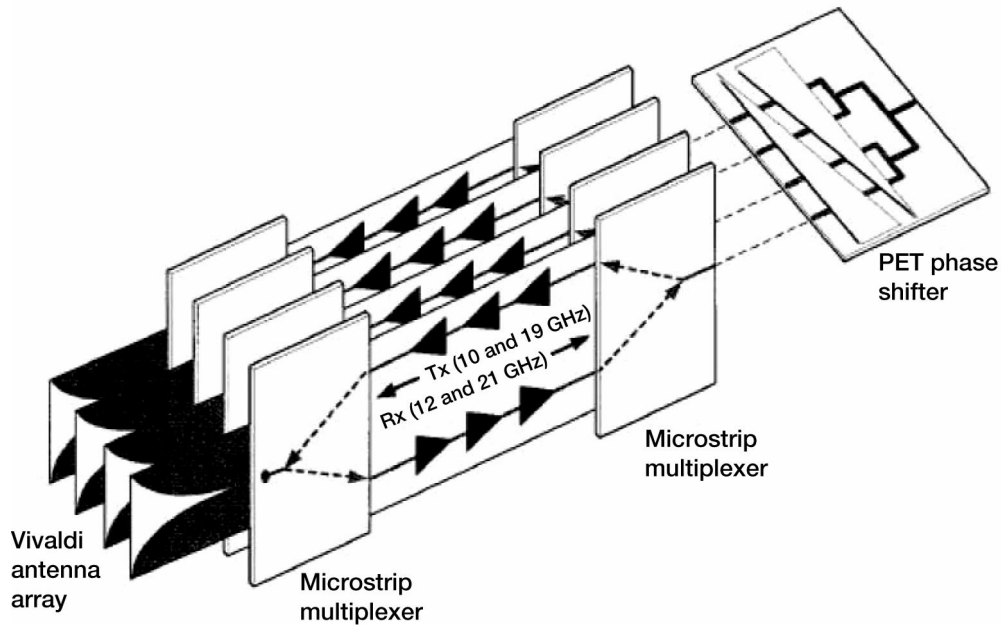


Figure 25.—Multi-frequency and full-duplex Vivaldi phased array system with dual-PET phase controls. From ref. 9 with permission from IEEE.



## Conclusion

The objective of this chapter is to provide an overview of notch antennas including underlying principles and limitations, general design guidelines, performance characteristics, and new applications. Due to limited coverage, the chapter focuses mainly on LTSA and Vivaldi, while many other noteworthy works have not been able to include in the discussion. The general design guideline outlined in the chapter is intended as an initial step in the experimental or analytical processes leading to the final design. The discussions on feeding techniques and antenna characteristics are useful in understanding the design and the radiation process of the notch antennas. Finally, the chapter ends with some recent advances and innovative applications of TSA arrays based on shared aperture technology.

## References

- [1] L.R. Lewis, M. Fassett and J. Hunt, "A Broadband Stripline Array Element," *1974 IEEE AP-S International Symposium*, Atlanta, GA June 1974, pp. 335–337.
- [2] Ramakrishna Janaswamy, "An accurate Moment Method Model for the Tapered Slot Antenna," *IEEE Trans. Antenna and Propagation*, Vol. 37, No. 12, December 1989, pp. 1523–1528.
- [3] Eric Thiele and Allen Taflove, "FD–TD Analysis of Vivaldi Flared Horn Antennas and Arrays," *IEEE Trans Antenna and Propagation*, Vol. 42, No. 5, May 1994, pp. 633–641.
- [4] Liang-Chen Kuo, Meng-Chung Tsai and Huey-Ru Chang, "3–D FDTD Design Simulation and Experimental Measurement of a Ka-Band Planar Antipodal Linearly-Tapered Slot Antenna (ALTSA)," *IEEE Microwave and Wireless Components Letters*, Vol. 11, No. 9, Sept. 2001, pp. 382–384.
- [5] "CAD Benchmark on a Balanced Antipodal Vivaldi Antenna," *Microwave Engineering Europe* (<http://www.mwee.com/magazine/2000/CAD-nov.htm>), October 2000.
- [6] Nai-Shuo Cheng, Pengcheng Jia, David B. Rench and Robert A. York, "A 120-W X–Band Spatially Combined Solid-State Amplifier," *IEEE Trans. Microwave Theory and Techniques*, Vol. 47, No. 12, Dec. 1999, pp. 2557–2559.
- [7] T.L. Korzeniowski, D.M. Pozar, D.H. Schaubert, and K.S. Yngvesson, "Imaging System at 94 GHz Using Tapered Slot Antenna Elements," *Proceedings of the 8th International Conference on Infrared and Millimeter Waves*, 1983.
- [8] Hung Loui, Jan Peeters Weem and Zoya Popovic, "A Dual-Band Dual3-Polarized Nested Vivaldi Slot Array With Multilevel Ground Plane," *IEEE Trans. Antennas and Propagation*, Vol. 51, No. 9, September 2003, pp. 2168–2175.
- [9] Tae-Yeoul Yun, Chunlei Wang, Paola Zepeda, Christopher T. Rodenbeck, Mathew R. Coutant, Ming-yi Li, and Kai Chang, "A 10–21 GHz, Low-Cost, Multifrequency, and Full-Duplex Phased-Array Antenna System," *IEEE Trans AP-S*, Vol. 50, No. 5, May 2002, pp. 641–649.
- [10] Kai Fong Lee and Wei Chen, *Advances in Microstrip and Printed Antennas*, Wiley Interscience, New York 1997. Chapter 9, p. 443.
- [11] S.N. Prasad and S. Mahapatra, "A Novel MIC Slot Line Aerial," *Proc. 9th European Microwave Conf.*, Brighton, U.K. 1979, pp. 120–124.
- [12] P.J. Gibson, "The Vivaldi Aerial," *Proc., 9th European Microwave Conf.*, Brighton, U.K. 1979, pp. 101–105.

- [13] T.L. Hwang, D.B. Rutledge, and S.E. Schwarz, "Planar Sandwich Antennas for Submillimeter Applications," *Appl. Phys. Lett.* Vol. 34 (1), 1 January 1979, pp. 9–11
- [14] R.N. Simons, N.I. Dib, R.Q. Lee, and L.P.B. Katehi, "Integrated Uniplanar Transition for Linearly Tapered Slot Antenna," *IEEE Trans. Antennas and Propagation*, Vol. 43, No. 9, 1995, pp. 998–1002.
- [15] J.J. Lee and S. Livingston, "Wide Band Bunny-Ear Radiating Element," *1993 IEEE AP-S International Symposium Digest*, June 1993, pp. 1604-1607.
- [16] E. Gazit, "Improved Design of the Vivaldi Antenna," *IEE Proc., Part H*, Vol. 135, No. 2, 1988, pp. 89–92.
- [17] J.D.S. Langley, P.S. Hall, and P. Newham, "Balanced Antipodal Vivaldi Antenna for Wide Bandwidth Phased Arrays," *IEE Proc. Antennas Propag.*, Vol. 143, No. 2, April 1996, pp. 97–102.
- [18] X.D. Wu and K. Chang, "Compact Wideband Integrated Active Slot Antenna Amplifier," *Elect. Lett.* Vol. 29, No.5, March 1993, pp. 496–497.
- [19] Guiping Zheng, Ahmed A. Kishk, Allen W. Glisson, and Alexander B. Yakovlev, "Slot Antenna Fed by a CPW Line with Tapered Transition," *Microwave and Optical Tech. Lett.*, Vol. 38, No. 6, September 2003, pp. 465–467.
- [20] I. Linardou and C. Migliaccio, "Twin Vivaldi Antenna for Transponders and Monopulse Systems," *Microwave and Optical Technology Letters*, Vol. 27, No. 3, Nov. 2000, pp. 207–209.
- [21] N. Marchand, "Transmission Line Conversion," *Electronics*, Vol. 17, 1944, pp. 142–145.
- [22] A.B. Smolders and M.J. Arts, "Wide-Band Antenna Element with Integrated Balun," *1998 IEEE AP-S Int. Symposiums Digest*, Atlanta, USA, June 1998.
- [23] V. Trifunovic and B. Jokanovic, "Review of Printed Marchand and Double-Y Baluns: Characteristics and Application," *IEEE Trans. On Microwave Theory and Techniques*, Vol. 42, No. 8, Aug. 1994, pp. 1454–1462.
- [24] R.N. Simons, N.I. Dib, R.Q. Lee, and L.P.B. Katehi, "Integrated Uniplanar Transition for Linearly Tapered Slot Antenna," *IEEE Trans. Antennas Propagation*, Vol. 43, No. 9, 1995, pp. 998–1002.
- [25] R.N. Simons, R.Q. Lee, and T.D. Perl, "Non-Planar Linearly Tapered Slot Antenna with Balanced Microstrip Feed," *1992 IEEE AP-S International Symposium*, Vol. 4, 1992, pp. 2109–2112.
- [26] P. Knott and A. Bell, "Coaxially-Fed Tapered Slot Antenna," *Electronics Letters*, Vol. 37, No. 18, Aug. 2001, pp. 1103–1104.
- [27] K. Sigfrid Yngvesson, T.L. Korzeniowski, Young-Sik Kim, Erik L. Kollberg, and Joakim F. Johansson, "The Tapered Slot Antenna—A New integrated Element for Millimeter-Wave Application," *IEEE Trans. Microwave and Techniques*, Vol. 37, No. 2, Feb. 1989, pp. 365–374.
- [28] T. Thungren, E.L. Kollberg and K.S. Yngvesson, "Vivaldi Antennas for Single Beam Integrated Receiver," *Proceedings of the 12th European Microwave Conference*, 1982, pp. 475–480.
- [29] P.S. Kooi, T.S. Yeo, and M.S. Leong, "Parametric Studies of the Linearly Tapered Slot Antenna (LTSA)," *Microwave and Optical Tech. Lett.*, Vol. 4, No. 5, April 1991, pp. 200–206.
- [30] D.C. Hogg and W.E. Legg, "A Finline Radiator," *The Bell System Technical Journal*, Vol. 52, No. 7, September 1973, pp. 1249–1253.
- [31] J.S. Colbum and Y. Rahmat-Samii, "Printed Antenna Pattern Improvement Through Substrate Perforation of High Dielectric Constant Material: An FDTD Evaluation," *Microwave and Optical Technology Letters*, Vol. 18, No. 1, May 1998, pp. 27–32.

- [32] Thomas J. Ellis and Gabriel M. Rebeiz, "MM-Wave Tapered Slot Antennas on Micromachined Photonic Bandgap Dielectrics," *1996 IEEE MTT-S International Symposium Digest*, pp. 1157–1160.
- [33] K.S. Yngvesson, D.H. Schaubert, T.L. Korzeniowski, E.L. Kolberg, T. Thungren, and J.F. Johnson, "Endfire Tapered Slot Antennas on Dielectric Substrate," *IEEE Trans. Antennas Propagat.*, Vol. 33, No. 12, 1985, pp. 1392-1400.
- [34] R.N. Simons and R.Q. Lee, "Linearly Tapered Slot Antenna Impedance Characteristics," *1995 IEEE AP-S International Symposium Digest*, Vol. 1, 1995, pp. 170–173.
- [35] NIST De-embedding software, *Program DEEMBED*, Rev. 4.04, 1994.
- [36] R.N. Simons and R.Q. Lee, "Characterization of Miniature Millimeter-Wave Vivaldi Antenna for Local Multipoint Distribution Service," *49th ARFTG/MTT Conference Digest*, 1997, pp. 95–99.
- [37] R.N. Simons and R.Q. Lee, "On-Wafer Characterization of Millimeter-Wave Antennas for Wireless Applications," *IEEE Trans. Microwave Theory and Techniques*, Vol. 47, No. 1, Jan. 1999, pp. 92–96.
- [38] R.N. Simons and R.Q. Lee, "Space Power Amplification with Active Linearly Tapered Slot Antenna Array," *Proceedings of the 1993 IEEE MTT-S International Microwave Symposium*, Vol. II, pp. 623–626.
- [39] R.N. Simons and R.Q. Lee, "Spatial Frequency multiplier with Active Linearly Tapered Slot Antenna Array," *Proceedings of the 1994 IEEE MTT-S International Microwave Symposium*, Vol. III, pp. 1557–1560.
- [40] R.N. Simons, E. Kelly, R.Q. Lee, and S.R. Taub, "Radial Microstrip Slotline Feed Network for Circular Mobile Communications Array," *1994 IEEE AP-S International Symposium Digest*, Vol. 2, pp. 1024–1027.
- [41] M.J. Vaughan and R.C. Compton, "28 GHz Omni-Directional Quasi-Optical Transmitter Array," *IEEE Trans. Microwave Theory and Techniques*, Vol. 43, No. 10, 1995, pp. 2507–2509.
- [42] Bernhard Schoenlinner, Xidong Wu, Jim P. Ebling, George V. Eleftheriades, and Gabriel M. Rebeiz, "Wide-Scan Spherical-Lens Antennas for Automotive Radars," *IEEE Trans. on Microwave Theory and Techniques*, Vol. 50, No. 9, Sept. 2002, pp. 2166–2175.
- [43] T.A. Axness, R.V. Coffman, B.A. Kopp, and K.W. O'Haver, "Shared Aperture Technology Development," *Johns Hopkins APL Technical Digest*, Vol. 17, No. 3, 1996, pp. 285–294.

<b>REPORT DOCUMENTATION PAGE</b>			<i>Form Approved</i> <i>OMB No. 0704-0188</i>	
Public reporting burden for this collection of information is estimated to average 1 hour per response, including the time for reviewing instructions, searching existing data sources, gathering and maintaining the data needed, and completing and reviewing the collection of information. Send comments regarding this burden estimate or any other aspect of this collection of information, including suggestions for reducing this burden, to Washington Headquarters Services, Directorate for Information Operations and Reports, 1215 Jefferson Davis Highway, Suite 1204, Arlington, VA 22202-4302, and to the Office of Management and Budget, Paperwork Reduction Project (0704-0188), Washington, DC 20503.				
<b>1. AGENCY USE ONLY (Leave blank)</b>		<b>2. REPORT DATE</b> July 2004	<b>3. REPORT TYPE AND DATES COVERED</b> Technical Memorandum	
<b>4. TITLE AND SUBTITLE</b>  Notch Antennas			<b>5. FUNDING NUMBERS</b>  WBS-22-302-20-1D	
<b>6. AUTHOR(S)</b>  Richard Q. Lee				
<b>7. PERFORMING ORGANIZATION NAME(S) AND ADDRESS(ES)</b>  National Aeronautics and Space Administration John H. Glenn Research Center at Lewis Field Cleveland, Ohio 44135-3191			<b>8. PERFORMING ORGANIZATION REPORT NUMBER</b>  E-14503	
<b>9. SPONSORING/MONITORING AGENCY NAME(S) AND ADDRESS(ES)</b>  National Aeronautics and Space Administration Washington, DC 20546-0001			<b>10. SPONSORING/MONITORING AGENCY REPORT NUMBER</b>  NASA TM-2004-213057	
<b>11. SUPPLEMENTARY NOTES</b>  Responsible person, Richard Q. Lee, organization code 5640, 216-433-3489.				
<b>12a. DISTRIBUTION/AVAILABILITY STATEMENT</b>  Unclassified - Unlimited Subject Category: 32  Available electronically at <a href="http://gltrs.grc.nasa.gov">http://gltrs.grc.nasa.gov</a> This publication is available from the NASA Center for AeroSpace Information, 301-621-0390.			<b>12b. DISTRIBUTION CODE</b>	
<b>13. ABSTRACT (Maximum 200 words)</b>  Notch antennas, also known as the tapered slot antenna (TSA), have been the topics of research for decades. TSA has demonstrated multi-octave bandwidth, moderate gain (7 to 10 dB), and symmetric E- and H- plane beam patterns and can be used for many different applications. This chapter summarizes the research activities on notch antennas over the past decade with emphasis on their most recent advances and applications. This chapter begins with some discussions on the designs of single TSA; then follows with detailed discussions of issues associated with TSA designs and performance characteristics. To conclude the chapter, some recent developments in TSA arrays and their applications are highlighted.				
<b>14. SUBJECT TERMS</b>  Slot antenna; Antenna array; Antenna design			<b>15. NUMBER OF PAGES</b> 29	
			<b>16. PRICE CODE</b>	
<b>17. SECURITY CLASSIFICATION OF REPORT</b> Unclassified	<b>18. SECURITY CLASSIFICATION OF THIS PAGE</b> Unclassified	<b>19. SECURITY CLASSIFICATION OF ABSTRACT</b> Unclassified	<b>20. LIMITATION OF ABSTRACT</b>	



